

NIGHT SKY BRIGHTNESS AT SAN PEDRO MARTIR OBSERVATORY

I. PLAUCHU-FRAYN¹, M. G. RICHER¹, E. COLORADO¹, J. HERRERA¹, A. CÓRDOVA¹, U. CESEÑA¹, F. ÁVILA.¹

Accepted to Publications of the Astronomical Society of the Pacific

ABSTRACT

We present optical UBVRI zenith night sky brightness measurements collected on eighteen nights during 2013–2016 and SQM measurements obtained daily over twenty months during 2014–2016 at the Observatorio Astronómico Nacional on the Sierra San Pedro Mártir (OAN-SPM) in México. The UBVRI data is based upon CCD images obtained with the 0.84m and 2.12m telescopes, while the SQM data is obtained with a high-sensitivity, low-cost photometer. The typical moonless night sky brightness at zenith averaged over the whole period is $U = 22.68$, $B = 23.10$, $V = 21.84$, $R = 21.04$, $I = 19.36$, and $SQM = 21.88$ mag arcsec⁻², once corrected for zodiacal light. We find no seasonal variation of the night sky brightness measured with the SQM. The typical night sky brightness values found at OAN-SPM are similar to those reported for other astronomical dark sites at a similar phase of the solar cycle. We find a trend of decreasing night sky brightness with decreasing solar activity during period of the observations. This trend implies that the sky has become darker by $\Delta U = 0.7$, $\Delta B = 0.5$, $\Delta V = 0.3$, $\Delta R = 0.5$ mag arcsec⁻² since early 2014 due to the present solar cycle.

Subject headings: atmospheric effects – light pollution – site testing – techniques: photometric – zodiacal dust

1. INTRODUCTION

The Observatorio Astronómico Nacional San Pedro Mártir (hereafter OAN-SPM) is located on the top of Sierra San Pedro Mártir in Baja California, México (2800m, +31° 02′ 40′ N, 115° 28′ 00′ W). The site excels in sky clarity with, in recent decades, approximately 70% and 80% photometric and spectroscopic time, respectively (Tapia et al. 2007). The median seeing measured at zenith at 5000Å varies from 0.″50 to 0.″79 (Echevarría et al. 1998; Michel et al. 2003; Skidmore et al. 2009; Sánchez et al. 2012). Atmospheric extinction is typically 0.13 mag airmass⁻¹ in V band (Schuster and Parrao 2001). Due to these excellent atmospheric conditions and favorable location away from large urban areas, the OAN-SPM is an excellent site for optical and infrared facilities.

Among the most important parameters that define the quality of an observing site it is the night sky brightness (NSB). This parameter has been extensively studied by several authors (Kalinowski et al. 1975; Walker 1988; Pilachowski et al. 1989; Krisciunas et al. 1987; Leinert et al. 1995; Mattila et al. 1996; Patat 2003 and references therein), starting with the pioneering work by Rayleigh (1928). In the following, we will concentrate on optical wavelengths only.

The NSB is the integrated light from two main kinds of sources: natural and artificial. Among the sources of natural origin are airglow (recombination of molecules heated by Sun UV radiation during daytime), aurorae, zodiacal light (sunlight scattered from interplanetary dust), diffuse galactic light (from faint unresolved stars in our Galaxy), and the extragalactic background (due to distant, faint unresolved galaxies). The airglow and

aurorae, which originate in the Earth’s atmosphere, depend upon the site and time of the observation, while the other three do not. The source of artificial light is mainly street lighting, with an increasing contribution from electronic billboards and other luminous advertising media. This contribution, also known as light pollution, is amenable to monitoring through long-term campaigns of the variation in the night sky brightness (Schneeberger et al. 1979; Walker 1988; Kalinowski et al. 1975; Krisciunas et al. 1987; Pilachowski et al. 1989; Leinert et al. 1995).

In Fig. 1 we show the cities and towns near the OAN-SPM. The cities of Ensenada and Tijuana lie between 150 and 230 km NW of OAN-SPM and have populations of 480,000 and 1.6 million people, respectively. The city of San Diego lies 260 km distant, also to the NW, with a population of 1.3 million people. An estimate of the contribution to the NSB due to light from nearby cities can be obtained using the model of Garstang (1989), which provides an approximate light-pollution contribution expected from different sources. The combined contribution of Ensenada, Tijuana and San Diego to the sky brightness at the OAN-SPM is estimated to be less than 0.08 mag at a zenith distance of 45°. To the Northeast, at an average distance of 185 km, the cities of Mexicali, Yuma, and San Luis Río Colorado, with a combined population of 1.3 million contribute with 0.04 mag. Other cities like San Felipe and San Quintín, which are nearer to the observatory (~60 km), but less populated (~17 000 and 10 000 people) contribute <0.01 mag each. In Baja California, state lighting ordinances that took effect starting in 2006 in the municipality of Ensenada and statewide in 2010 include light pollution among the environmental disturbances to be controlled. Among its goals, this legislation seeks to reduce or at least minimize the light pollution, even with the constant growth of its cities.

¹ Instituto de Astronomía, Universidad Nacional Autónoma de México, Apartado Postal 106, 22800 Ensenada, B.C., México.

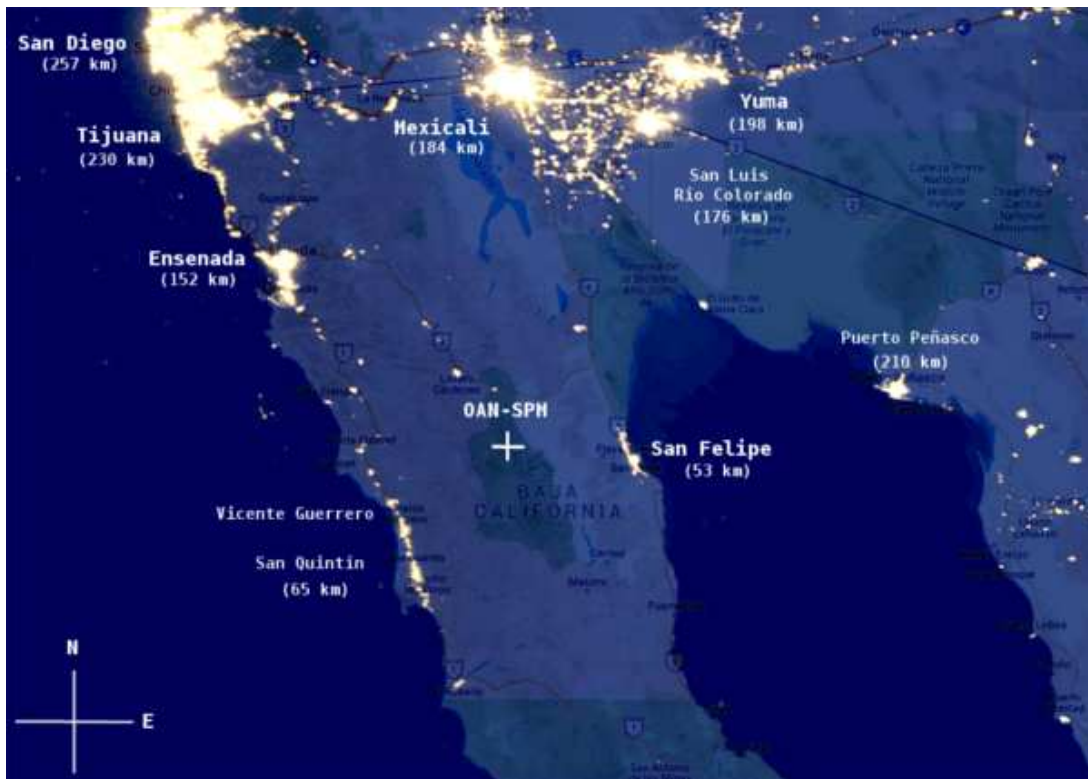


FIG. 1.— Night map showing nearby cities and their approximate distances to OAN-SPM. The cross indicates the location of the OAN-SPM. Bright areas indicate street lights as seen from space. Credit: Google maps and NightEarth.com with data provided by NASA.

In the present paper we report UBVR_I sky brightness measurements obtained on eighteen moonless nights during 2013 to 2016 and SQM sky brightness measurements collected daily during 2014 to 2016. As far as we are aware, these data constitute the largest homogeneous data set available for the OAN-SPM. The SQM data set is continuously accumulating and it will provide an unprecedented opportunity to investigate the long-term evolution of the night sky at the OAN-SPM. In Sect. 2, we present our observation procedures and reduction techniques. The results are presented in Sect. 3, while, in Sect. 4, we consider the variation of the NSB as a function of the solar activity and compare our measurements with other dark sites. Finally, in Sect. 5, we present our conclusions.

2. OBSERVATIONS AND DATA REDUCTION

2.1. CCD night sky brightness measurements

The broadband data set presented in this study was obtained with the MEXMAN and Italian filter wheels, which are mounted at the Cassegrain focus of the 0.84 m and 2.1 m Ritchey-Chretien telescopes, respectively. The detectors are E2V back-illuminated CCDs with $13.5\ \mu\text{m}$ pixels in a 2048×2048 format, which give projected plate scales of $0''.22/\text{pix}$ and $0''.18/\text{pix}$ at the 0.84 m and 2.1 m telescopes, respectively.

Observations of the NSB were obtained at the zenith to minimize airglow emission and extinction on 18 photometric nights between February 2013 to May 2016 when both the Sun and Moon were at least 18° below the horizon (astronomical night). Each night, a

photometric standard field (Landolt 1992) was observed at about the same time as part of the calibration process.

Imaging frames are bias and flat-field corrected using standard reduction procedures in IRAF². Average integration times range between 600s in U band and 300s in I band, in order to obtain sufficient sky counts. Aperture photometry was performed with the APT software (Laher et al. 2012) by using an aperture of $13''$ in areas free of nebulousity, stars, and cosmic rays. The instrumental magnitudes of the standard stars were corrected for atmospheric extinction, using the standard values for the OAN-SPM (Schuster and Parrao 2001). No color correction was applied to these magnitudes. Following the prescriptions of Pilachowski et al. (1989), the NSB is calibrated without correcting for atmospheric extinction because we are interested in the observed brightness. The typical average uncertainty in the photometry, neglecting the uncertainty in the exposure time and aperture size, in our NSB measurements are 0.13, 0.05, 0.04, 0.03 and 0.02 mag for U, B, V, R, and I bands, respectively, based upon image statistics. Our complete NSB data set from CCD imaging is tabulated in Table 7.

The NSB has an important contribution from zodiacal light that has to be taken into account. In Fig. 2, we show an image of the all-sky camera installed at the OAN-SPM for the night of 18 February 2015 where we

² IRAF is distributed by the National Optical Astronomy Observatory, which is operated by AURA, INC. under cooperative agreement with the National Science Foundation

may appreciate the presence of the Milky Way at the zenith and the zodiacal light to the SW on the horizon. In Fig. 3, we have superimposed the telescope pointings on a contour plot of the zodiacal light V brightness in helio-ecliptic coordinates (Levasseur-Regourd and Dumont 1980), i.e., ecliptic latitude versus the difference in ecliptic longitude of the observation and that of the Sun. We have used the equatorial celestial coordinates at the zenith when the sky brightness was measured and converted the right ascension and declination to helio-ecliptic coordinates. The surface brightness contours are expressed in surface brightness units, sbu ($\text{erg s}^{-1} \text{cm}^{-2} \text{\AA}^{-1} \text{sr}^{-1}$), e.g., a typical V sky brightness of $21.6 \text{ mag arcsec}^{-2}$ is equivalent to 366 sbu . The spectrum of the zodiacal light is very similar to that of the Sun over the UV-IR range, and peaks at 4500 \AA . In order to reduce the scatter in our NSB measurements, we remove the zodiacal light contribution in the UBVRi passbands for each telescope pointing (see Table 7 for the individual corrections). The average contribution to the total NSB is 45%, 60%, 25%, 10%, and 4% in the U, B, V, R, and I bands, respectively (see Table 1).

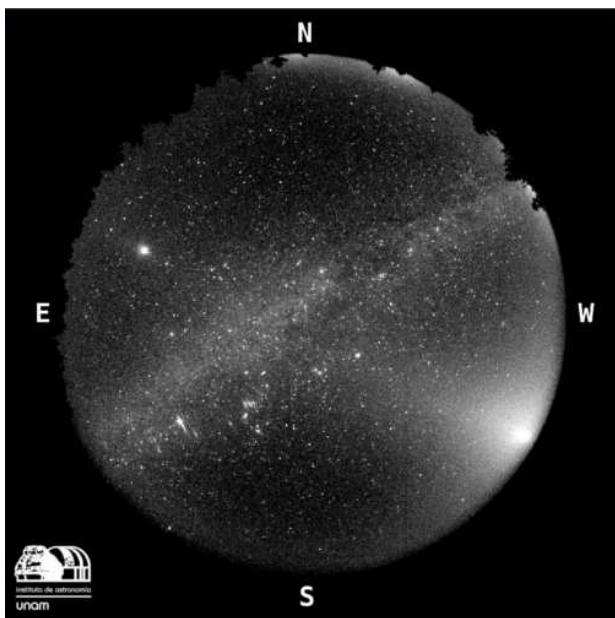


FIG. 2.— The Milky Way (center) and zodiacal light (SW) are seen clearly in this image taken by the All-sky camera at OAN-SPM on 18 February 2015.

2.2. SQM night sky brightness measurements

Since 2 November 2014, we have monitored the sky with an Unihedron Sky Quality Meter³ (hereafter SQM) in a continuous manner. This is a low cost NSB photometer with high enough sensitivity to quantify the quality of the night sky at any place. The SQM is encased in a weatherproof housing pointing at the zenith. Periodically, the housing is cleaned manually. Our study includes data spanning 607 nights from November 2014 to June 2016, of which 534 (88%) have

³ <http://www.unihedron.com>

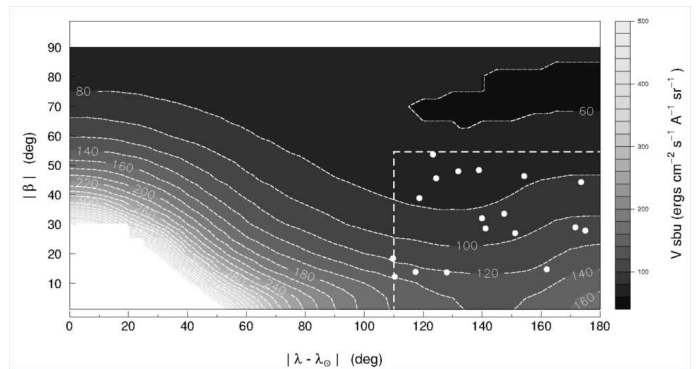


FIG. 3.— We superpose the distribution of the telescope pointings in helio-ecliptic coordinates (white circles) upon a contour plot of the zodiacal light in the V-band. The surface brightness of the zodiacal light is expressed in surface brightness units, sbu ($\text{erg s}^{-1} \text{cm}^{-2} \text{\AA}^{-1} \text{sr}^{-1}$). The region inside the box $|\lambda - \lambda_{\odot}| > 110^\circ$ and $|\beta| < 54.5^\circ$ (dashed line) contains the zenith pointings of the SQM in helio-ecliptic coordinates. Original data for zodiacal light contours are from Levasseur-Regourd and Dumont (1980).

available data. The SQM has a spectral response similar, though not identical, to the V band. Its sensitivity peaks at 5400 \AA with a broad transmittance window ($\sim 2000 \text{ \AA}$; see ? for a detailed comparison with standard photometric systems). Here, we follow the convention of other authors and report all measurements in terms of the SQM spectral band unit, $\text{mag}_{\text{SQM}} \text{ arcsec}^{-2}$.

The SQM measures the NSB every minute in a cone of about 20° (FWHM) and reports the result in astronomical units of magnitudes per square arcsecond with a precision of $0.1 \text{ mag arcsec}^{-2}$. Due to the large field of view, this device detects both the zenithal and near-zenithal NSB, underestimating the true NSB of the zenith (lower values, i.e. brighter magnitudes). This over-estimate is about $0 - 0.3 \text{ mag arcsec}^{-2}$, depending upon the light pollution at the site. Also, the SQM includes the integrated light from all stars within the field of view, which contribute approximately 6% of the NSB for stars of magnitude $\leq 5 \text{ mag}$ and must be accounted for (?). We do not apply corrections for either light pollution or the integrated light of stars.

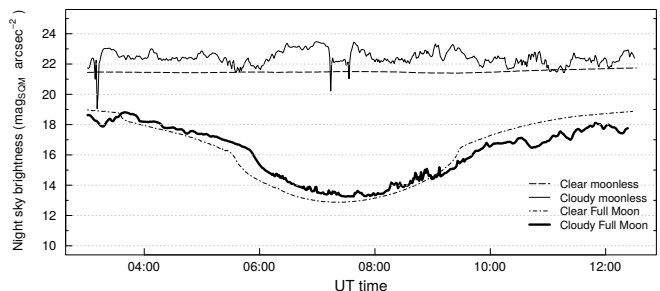


FIG. 4.— Examples of the variation in the SQM measurements under different conditions of cloud cover.

In Fig. 4, we present the SQM data plotted for four different nights: a cloudy moonless night, a clear moonless night, a clear moonlit night, and a cloudy moonlit night, in order to show the expected variations of the SQM data. The sky brightness on clear nights ranges

from the brightest value of $13 \text{ mag}_{SQM} \text{ arcsec}^{-2}$ (Full Moon at 30° from zenith), to $21.3 \text{ mag}_{SQM} \text{ arcsec}^{-2}$ (Galactic plane at the zenith), to the darkest value of $22 \text{ mag}_{SQM} \text{ arcsec}^{-2}$ on a moonless night. A rough estimate of the percentage of the night time (moonless and moonlit nights) free of clouds is found to be 74%, in accord with previous studies (e.g., [Tapia et al. 2007](#)).

We filter the data in several ways in order to minimize unnecessary light contributions from different sources. First, we only consider data obtained on nights that are entirely clear. This data has been chosen by visual inspection of All-sky camera images (see Fig. 2), resulting in 332 full nights. Second, we select only data taken during dark time, when the Sun and Moon are at least 18° below the horizon. Third, to minimize the corrections for zodiacal light, we restrict our observations to high helio-ecliptic longitudes. Since our data set lies at ecliptic latitudes $\leq 55^\circ$, we have applied a correction to all SQM measurements depending on their helio-ecliptic coordinates (see Col. 7 in Table 8) based upon the flux of the zodiacal light in the V band (see Fig. 3). The contribution of zodiacal light is almost constant for a given value of $|\beta|$ for $|\lambda - \lambda_\odot| > 110^\circ$, but it varies from 0.2 to 0.4 mag from $|\beta| = 0^\circ$ to $|\beta| = 55^\circ$. Finally, to avoid strong contributions from the Galactic plane, we have restricted our observations to galactic latitudes $|b| > 20^\circ$. As a result, we retain data from 183 nights with at least 10 measurements each.

Table 8 presents all our SQM measurements as well as the zodiacal light corrections we use for each measurement.

3. RESULTS

3.1. CCD results

In Table 1, we present the mean, minimum, and maximum values of the NSB before correction for zodiacal light (columns 2-4), while in the last two columns we present the values of the NSB corrected for zodiacal light (column 5) and the mean value of the zodiacal light contribution in each band (ΔZL , column 6). One can see from Col. 6 of Table 1 that the mean ΔZL is as large as 0.5 mag in the B passband, while for the other filters this correction is smaller. For detailed measurements of each eighteen nights and the zodiacal light correction in each filter and observing run we refer the reader to Table 7 and Fig. 12. As a by product of our CCD sky images we have also determined the sky colors, which we present in Table 2. The NSB and sky color uncertainties are the estimated internal error of a individual measurement by subtracting off the yearly averages from the data and computing the Gaussian standard deviation of the resultant distribution.

For two observing runs with Moon phase > 0.75 and zenith distance in the range of 40° – 60° , we have calculated the NSB and have found that this is on average brighter by 3.3, 3.8, 2.8, 2.1 and 0.7 magnitude in the U, B, V, R, and I bands, respectively. In Table 2 we also give the mean sky colors obtained on nine moonlit nights with Moon at zenithal distances in the

range of 40° – 60° and Moon phase > 0.75 .

3.2. SQM results

In Fig. 5 we show the NSB distribution as a function of Sidereal time before filtering for Galactic latitude or correcting for the zodiacal light contribution. At the latitude of OAN-SPM ($+31^\circ$), the galactic plane lies near Sidereal time 90° and 300° , where it can be seen that the NSB is brighter (i.e., lower values), with a contribution to the sky brightness of about 45% inside the field of view of the SQM due to the galactic plane.

On the other hand, in Fig. 6, we show the SQM data after filtering the data to retain only measurements made at high galactic latitude, $|b| \geq 20^\circ$, and after correcting for the zodiacal light contribution. The sky brightness variations are now dominated by the variability in the airglow and its patchy structure. The NSB variations in individual nights, from minimum to maximum values, range between 0.1 and $0.7 \text{ mag}_{SQM} \text{ arcsec}^{-2}$, with a mean value of $0.2 \pm 0.13 \text{ mag}_{SQM} \text{ arcsec}^{-2}$. On a given night, the NSB may increase, decrease, or remain constant with time. As found by [Walker \(1988\)](#), [Pilachowski et al. \(1989\)](#), and [Krisciunas \(1997\)](#), on any given night the sky brightness can vary 10% to 50%. The average dispersion of the NSB on a given night in our data is $\pm 0.06 \text{ mag}_{SQM} \text{ arcsec}^{-2}$ (Table 8, column 3).

The literature is mixed on whether and how the NSB varies as a function of the time after twilight. [Walker \(1988\)](#) pointed out that the sky at zenith gets darker by $\sim 0.4 \text{ mag arcsec}^{-2}$ during the first six hours after the end of twilight. On the other hand, [Krisciunas \(1990\)](#) found that his data obtained in the V passband showed a decrease of $\sim 0.3 \text{ mag arcsec}^{-2}$, but that this was not seen in the B passband. Other authors have not found evidence that the NSB decreases after twilight ([Leinert et al. 1995](#); [Mattila et al. 1996](#); [Benn and Ellison 1998](#); [Patat 2003](#)). Our data agree with these last results. In Fig. 7, we present the data set from Fig. 6, where we now plot the NSB as a function of UT time. From Fig. 7, it can be seen that there is no clear trend in NSB after twilight (local midnight at 08:00hrs UT), as found by the work previously cited.

Besides the variations of the NSB during a single night, there are night-to night and longer-term variations. In Fig. 8a, we present daily and monthly mean NSB, which show how the NSB can vary on short periods and to investigate any seasonal variation of the NSB. Although there is considerable variation, Fig. 8a shows that there is no evidence for any seasonal variation of the NSB, in the sense of a periodic variation. Instead, all the mean monthly values (black dots) are consistent with the global average given in Table 1 (last row) and shown with horizontal dashed lines in Fig. 8a. Fig. 8b presents the zodiacal light correction applied to the data in Fig. 8a (see Table 8). Meanwhile, in Fig. 8c, we plot the variation of the solar flux in the same period, which has been decreasing since 2014. The solar flux is expected to be correlated with the NSB (see Sect. 4.1). In Fig. 8d

TABLE 1
MEAN NIGHT SKY BRIGHTNESS AT OAN-SPM FROM 2013 TO 2016.

Filter	NSB $\pm\sigma$ (mag arcsec $^{-2}$)	NSB $_{min}$ (mag arcsec $^{-2}$)	NSB $_{max}$ (mag arcsec $^{-2}$)	NSB $_{ZL} \pm \sigma$ (mag arcsec $^{-2}$)	ΔZL (mag arcsec $^{-2}$)
<i>U</i>	22.27 \pm 0.21	21.56	22.84	22.68 \pm 0.20	0.41
<i>B</i>	22.60 \pm 0.15	22.05	23.26	23.10 \pm 0.12	0.50
<i>V</i>	21.59 \pm 0.12	21.05	22.11	21.84 \pm 0.11	0.25
<i>R</i>	20.90 \pm 0.12	20.36	21.46	21.04 \pm 0.12	0.14
<i>I</i>	19.32 \pm 0.17	18.81	19.90	19.36 \pm 0.16	0.04
<i>SQM</i>	21.62 \pm 0.16	21.10	22.04	21.88 \pm 0.15	0.26

Mean, minimum, and maximum NSB values not corrected for zodiacal light, the mean NSB corrected for zodiacal light, and the mean contribution of the zodiacal light for each filter. The σ is the estimated internal error of a individual measurement by subtracting off the yearly averages from the data and computing the Gaussian standard deviation of the resultant distribution.

TABLE 2
SKY COLORS AT OAN-SPM

Color	Moonless Mean $\pm \sigma$	Moonlit ^a Mean $\pm \sigma$
<i>U - B</i>	-0.323 \pm 0.174	-0.268 \pm 0.140
<i>B - V</i>	1.008 \pm 0.112	0.220 \pm 0.099
<i>V - R</i>	0.612 \pm 0.167	-0.003 \pm 0.024
<i>V - I</i>	1.521 \pm 0.370	0.415 \pm 0.194

The σ values are calculated as in Table 1.

^a Mean values for nine moonlit nights with Moon phase > 0.75 and zenithal distances of 40° – 60° (Sect. 3.3).

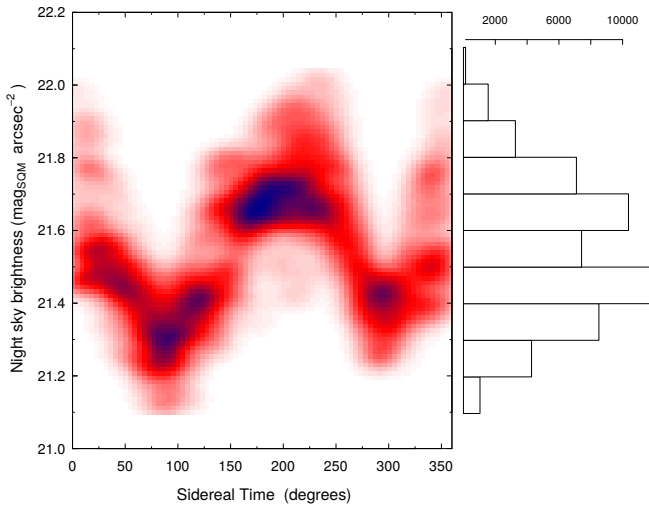


FIG. 5.— Distribution of the raw SQM measurements as a function of sidereal time (ST) for clear moonless nights. For demonstration purposes, the data have not been filtered to remove observations at low galactic latitude or corrected for the contribution of zodiacal light. At the latitude of the OAN-SPM, $+31^\circ$, the galactic plane lies at $ST \sim 90^\circ$ and $ST \sim 300^\circ$. The histogram shows the number of SQM measurements per bin of NSB (bin width is $0.1 \text{ mag}_{SQM} \text{ arcsec}^{-2}$). A bimodal distribution is produced due to light from the galactic plane.

we show the differences between CCD V band and SQM

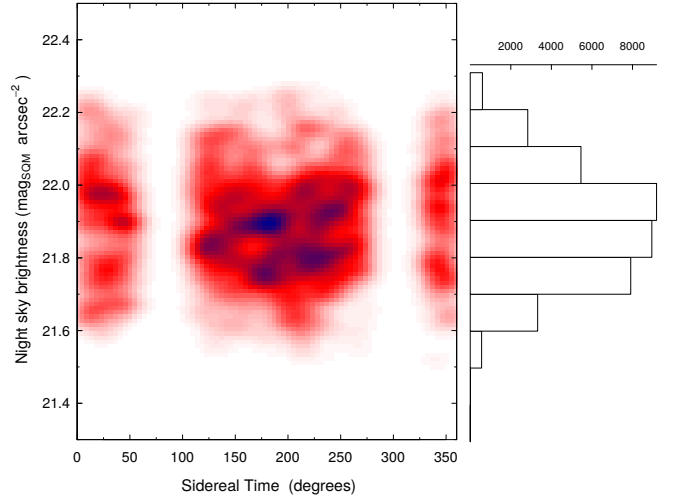


FIG. 6.— Distribution of the SQM measurements as a function of sidereal time for clear moonless nights. The data is filtered to remove observations at low galactic latitude and corrected to remove the contribution of zodiacal light. The histogram shows the number of SQM measurements per bin of NSB (bin width is $0.1 \text{ mag}_{SQM} \text{ arcsec}^{-2}$). Compared to Figure 5, the distribution of NSB values is now narrower and single-peaked.

measurements in order to check for any drift in the SQM sensor. From this figure it can be seen that SQM and CCD measurements are comparable, with no evidence of any drift.

3.3. Variation of the NSB with Moon phase and distance

As a by product of our SQM sky brightness measurements, we performed a quantitative analysis of the data when the Moon is above the horizon. (For this, we use the data filtered from Table 8.) In Fig. 9, we show the variation in the NSB as a function of Moon phase and zenithal distance.

As expected, we find a large increase in the NSB as the zenithal distance of the Moon decreases. This variation is naturally most extreme for the phase of full Moon. Figure 9 should be a useful tool for predicting the sky brightness enhancement produced by

TABLE 3
YEARLY NIGHT SKY BRIGHTNESS AT OAN-SPM

Filter	Year ^a			
	2013 NSB $\pm \sigma$ (mag arcsec ⁻²)	2014 NSB $\pm \sigma$ (mag arcsec ⁻²)	2015 NSB $\pm \sigma$ (mag arcsec ⁻²)	2016 NSB $\pm \sigma$ (mag arcsec ⁻²)
<i>U</i>	22.21 \pm 0.25	21.96 \pm 0.16	22.29 \pm 0.16	22.51 \pm 0.16
<i>B</i>	22.59 \pm 0.22	22.39 \pm 0.11	22.61 \pm 0.09	22.74 \pm 0.17
<i>V</i>	21.73 \pm 0.38	21.45 \pm 0.17	21.61 \pm 0.02	21.64 \pm 0.12
<i>R</i>	20.86 \pm 0.31	20.67 \pm 0.15	21.06 \pm 0.04	20.98 \pm 0.19
<i>I</i>	19.38 \pm 0.50	19.29 \pm 0.13	19.44 \pm 0.10	19.27 \pm 0.24
<i>SQM</i>	...	21.42 \pm 0.10	21.60 \pm 0.14	21.72 \pm 0.12
Flux _☉ ^b	115	152	116	96

^a The σ is estimated as in Table 1. NSB values are not corrected for zodiacal light.

^b Solar 10.7 cm flux units 1 sfu = 10^4 Jy = 10^{-22} W m⁻² Hz⁻¹.

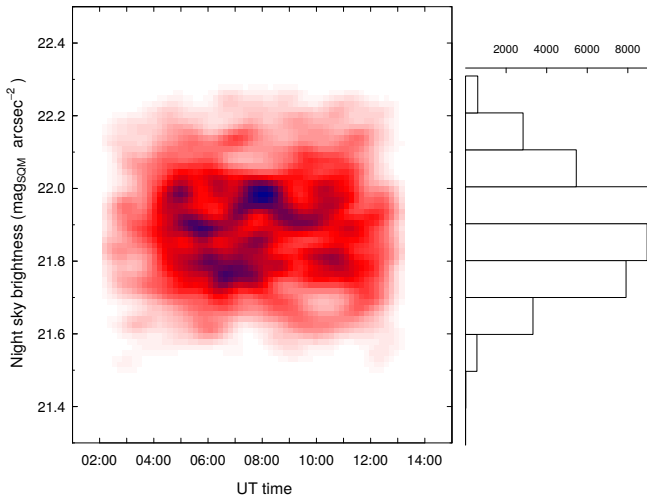


FIG. 7.— Distribution of the SQM measurements as a function of UT for clear moonless nights. The data is filtered to remove observations at low galactic latitude and corrected to remove the contribution for zodiacal light. The histogram shows the number of SQM measurements per bin of NSB (bin width is 0.1 mag_{SQM} arcsec⁻²).

the presence of the Moon at a given phase and angular distance from an observing target, at least in the V band. Taking into account the sky colors on moonlit nights presented in Table 2, one can see that the sky becomes bluer with the presence of the Moon. Hence, observations performed with filters bluer than V filter, will be more affected by the Moon than redder filters.

4. DISCUSSION

4.1. Correlation of the NSB with solar activity

A correlation between the intensity of the [O I] 5577 Å airglow line with the sunspot number was reported by Rayleigh (1928) and Rayleigh and Jones (1935). There is now a well-established correlation with solar activity for this and other emission lines, like [O I] 5777, 6300, 6364 Å, [O II] 7320, 7330 Å, Na D 5890, 5896 Å, and OH (Abreu et al. 1980; Yee et al. 1981; Takahashi et al. 1984). Walker (1988) also found that there is a correlation between the brightness of the for V and B

photometric bands with the solar 10.7 cm radio flux (an indicator of the solar activity), demonstrating that the correlation between sky brightness and solar activity applies not only for emission lines, but also for the airglow “pseudo continuum” emission. This correlation has been confirmed in other studies (Pilachowski et al. 1989; Leinert et al. 1995; Mattila et al. 1996; Krisciunas 1997).

In order to study this correlation with solar activity in our data, Table 3 presents the mean NSB for each year of our study. The last row of the table presents the solar 10.7 cm flux values “observed”, i.e., not corrected to 1 AU solar distance, and averaged over the months in which our NSB observations were made. The solar fluxes are public and provided by the Natural Resources Canada⁴. In Fig. 10, we plot the yearly average NSB values for the UBVRI filters and the SQM sensor for 2013–2016 against the solar 10.7 cm flux (solar flux unit; 1 sfu = 10^{-22} W m⁻² Hz⁻¹). We also shown the linear least squares fit to CCD data in each filter (solid lines) and SQM data (dotted line). Our data are from cycle #24 of the Sun, whose maximum was in early 2014. The Sun’s activity has been decreasing since then, so we might expect the sky to be darker for the next five years as the Sun passes through the minimum in the current cycle.

In Table 4 we present the parameters for the least squares fits shown in Fig. 10, with values of the NSB in each filter and the solar 10.7 cm flux, Flux_☉, taken from Table 3. The correlations in Table 4 indicate that there is a trend in which the NSB in the UBVRI and SQM bands ($|r| > 0.7$) decreases as the solar activity decreases (i.e., lower solar flux), as has been found previously. These trends have a high statistical significance ($P < 0.05$) only for the UB and SQM bands. The U and B bands are nearly devoid of emission lines from the sky. That the significance is lower for the VR bands compared to the SQM-band data is likely the result of the much larger number of data averaged in the latter case, given that the slopes are similar in the

⁴ <http://www.spaceweather.gc.ca>

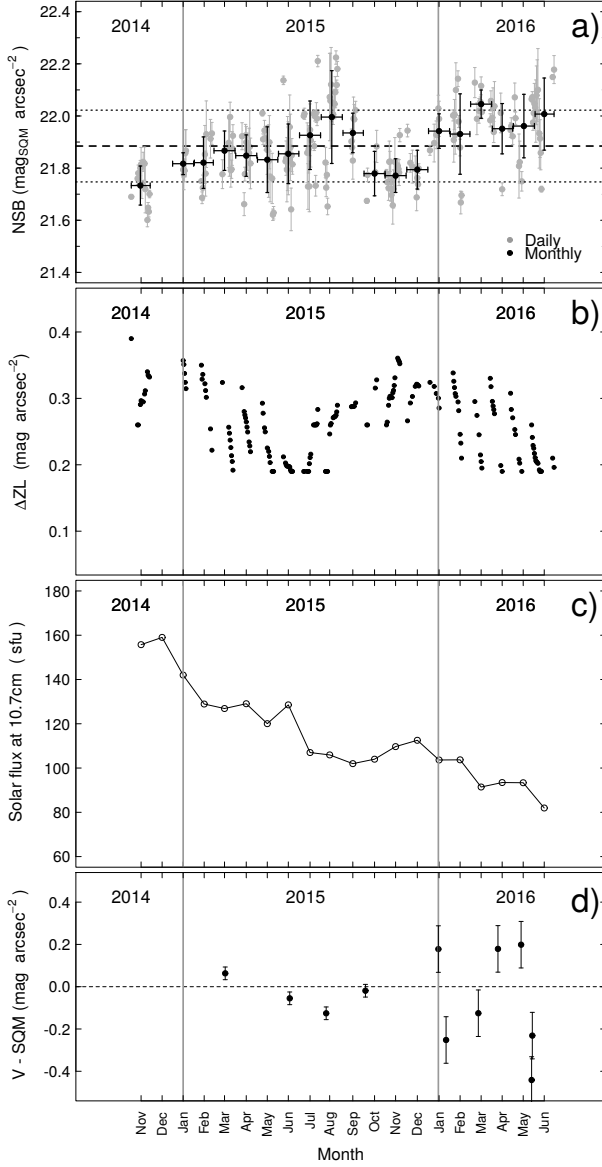


FIG. 8.— **a)** We present the SQM NSB measured at OAN-SPM from November 2014 to June 2016. The data were obtained on moonless nights, correcting for zodiacal light contributions, and excluding measurements near galactic plane, $|b| \geq 20^\circ$. The average daily (gray dots) and monthly (black dots) NSB values are shown. The global average value (dashed line; see last row Table 1) and the $\pm 1\sigma$ interval (dotted lines) are plotted. For the monthly NSB values, the vertical error bars are the standard deviation of the mean values, while horizontal error bars indicate the extent of one month. No significant seasonal behavior is found in this period. **b)** The zodiacal light contribution applied to NSB measurements. **c)** The monthly solar flux variation. **d)** We plot the difference between CCD V-band and SQM measurements as a function of time. We use the monthly mean value of mag_{SQM} , since we do not always have a nightly measurement for each date with UBVRI data. In all panels the vertical lines indicate the start and end of the year 2015.

three cases.

Since 1947, the minimum and maximum of the monthly average solar 10.7 cm flux are approximately 60 and 250 sfu ⁵. If we consider these extreme values

⁵ Monthly averages from 1947 to 2016 reported by the Natural Resources Canada.

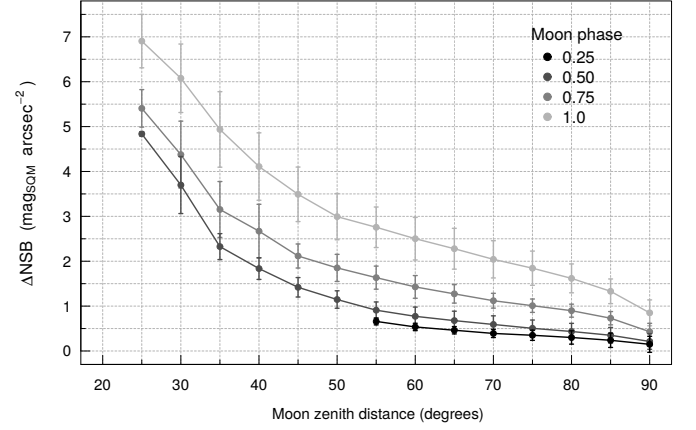


FIG. 9.— We plot the mean NSB measured with the SQM as a function of Moon phase and zenith distance. The error bars represent the standard deviation of the measurements. The NSB at zenith depends sensitively on both Moon phase and zenith distance.

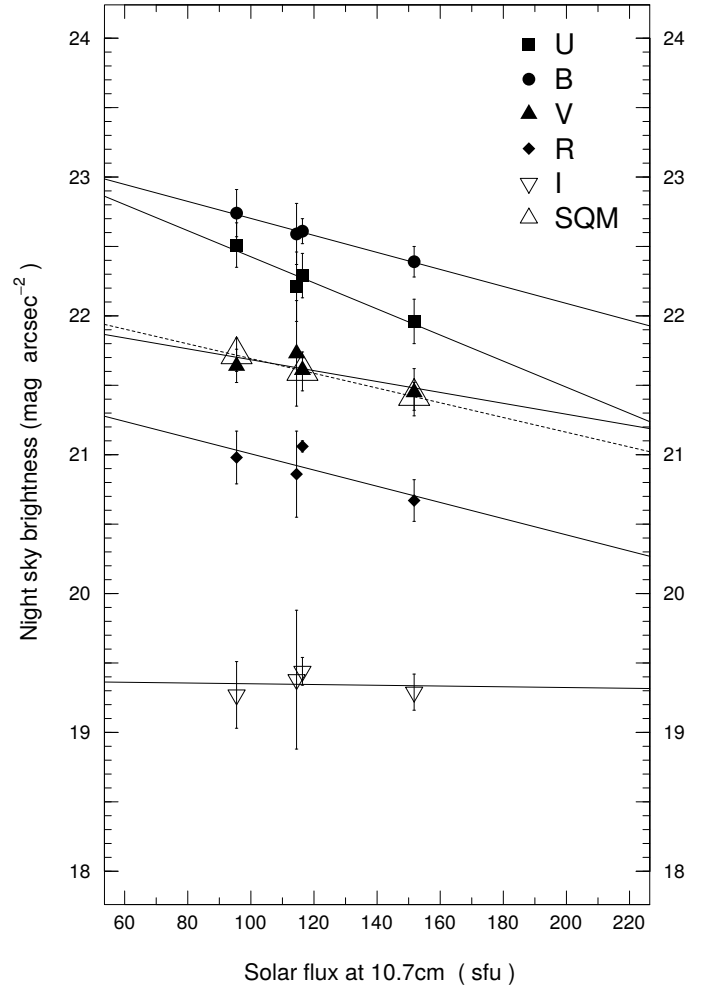


FIG. 10.— We plot the yearly averages of UBVRI bands and SQM night sky brightness as a function of time (2013-2016). The abscissa values are the averages of the solar 10.7 cm flux for those months when the NSB was measured. Lines represent fits to each band (solid line for CCD data and dotted line for SQM data). The detailed fit parameters are presented in Table 4.

and the slopes reported in Table 4, the total variation

TABLE 4
CORRELATIONS OF NSB WITH SOLAR
ACTIVITY

Filter	a	b	r	P
<i>U</i>	−0.009	23.37	−0.97	0.03
<i>B</i>	−0.006	23.31	−0.99	0.01
<i>V</i>	−0.004	22.08	−0.79	0.21
<i>R</i>	−0.006	21.59	−0.81	0.19
<i>I</i>	−0.0003	19.38	−0.08	0.92
<i>SQM</i>	−0.005	22.22	−0.99	0.02

a and b are the slope and intercept, respectively, of the linear fit, $NSB = a \times Flux_{\odot} + b$, r is the correlation coefficient, and P is the probability of obtaining the result by chance.

in NSB due to the solar activity over a complete cycle would be 1.8, 1.2, 0.7, and 1.1 mag in the UBVR bands, respectively, and 0.9 mag for SQM band. The current solar cycle has been less active, varying from a maximum of approximately 162 sfu in early 2014 to 82 sfu in recent months. This implies that, since early 2014, the NSB at the OAN-SPM has decreased by $\Delta U = 0.7$, $\Delta B = 0.5$, $\Delta V = 0.3$, $\Delta R = 0.5$ and $\Delta mag_{SQM} = 0.4$ mag arcsec^{−2}, respectively, based upon the slopes in Table 4.

4.2. Comparison with other observing sites

When comparing our measurements with the NSB from other observatories, we must account for the solar activity at the time all of the measurements were made. In Table 5, we compare our minimum and maximum NSB obtained in 2014 and 2016, respectively (see Table 3), at the OAN-SPM with broad band UBVR values available in the literature for other observatories. In Fig. 11, we plot the data for the BV bandpasses from Table 5. This presentation shows that the NSB measured at all of these sites are similar once account is taken of the solar activity.

In Fig. 11, we also show a linear fit to the data in order to determine the expected variation of the NSB due to solar activity. The fit parameters, correlation coefficients, and probability that they arise by chance are presented in Table 6. Although there is a lot of scatter, the large number of points lead to a robust fit. The dispersion about the fits in Table 6 is not surprising, as it is similar to that found in the monthly time bins in our SQM data (Fig. 8 and Table 8). From Table 6, we estimate a maximum variation over a solar cycle of 0.6 mag and 0.9 mag in the B and V bands, respectively, supposing that the solar activity varies from a minimum of 60 sfu to a maximum of 250 sfu.

TABLE 6
CORRELATIONS OF NSB WITH SOLAR ACTIVITY
FOR DATA IN FIG. 11

Filter	a	b	r	P	σ
<i>B</i>	−0.003	23.07	−0.57	0.02	0.27
<i>V</i>	−0.005	22.25	−0.76	0.0004	0.33

Columns 2 through 5 present, the slope (a), intercept (b), correlation coefficient (r), and the probability (P) for the least-squares fit of a linear relation for each filter, $NSB = a \times Flux_{\odot} + b$. Column 6 presents the standard deviation (σ) about this fit.

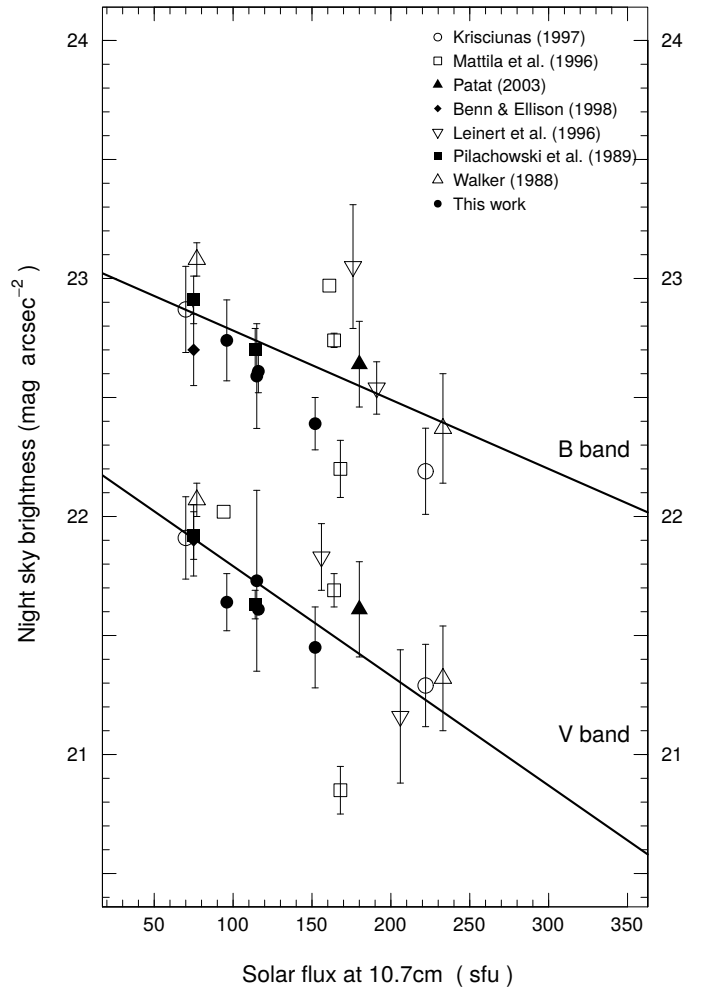


FIG. 11.— We compare the NSB at different observing sites as a function of the solar activity. The correlation seen here is very similar to that in Figure 10.

5. SUMMARY AND CONCLUSIONS

We obtained UBVR photometry of the night sky brightness (NSB) during 18 nights from 2013 to 2016 and SQM measurements on a daily basis from 2014

TABLE 5
COMPARISON OF ZENITH SKY BRIGHTNESS AT DIFFERENT SITES.

Site	NSB _U	NSB _B	NSB _V	NSB _R	NSB _I	Flux _☉ ^a (sfu)	Ref.
OAN-SPM	21.96	22.39	21.45	20.67	19.29	152	1
	22.51	22.70	21.64	20.98	19.27	96	
Hawaii	...	22.19	21.29	222	2
	...	22.87	21.91	70	
La Silla	...	22.20	20.85	168	3
	...	22.72	21.69	164	
	...	22.97	161	
	22.02	94	
Paranal	22.28	22.64	21.61	20.87	19.71	180	4
La Palma	22.00	22.70	21.90	21.00	20.00	75	5
Calar Alto	21.16	206	6
	...	22.54	191	
	...	23.05	176	
	21.83	156	
Kitt Peak	...	22.70	21.63	114	7
	...	22.91	21.92	75	
San Benito Mt.	...	22.37	21.32	233	8
	...	23.08	22.07	77	

NSB values are not corrected for zodiacal light contribution.

^a Solar 10.7 cm flux units 1 sfu = 10^4 Jy = 10^{-22} W m⁻² Hz⁻¹.

(1) This work; (2) Krisciunas (1997); (3) Mattila et al. (1996); (4) Patat (2003); (5) Benn and Ellison (1998); (6) Leinert et al. (1995); (7) Pilachowski et al. (1989); (8) Walker (1988).

to 2016 at the Observatorio Astronómico Nacional on the Sierra San Pedro Mártir (OAN-SPM). We have taken into account contributions to the sky brightness due to zodiacal light and have excluded observations at low galactic latitudes in order to compare our data to those obtained at other sites. We find no clear trend of the NSB as a function of time after twilight. The dispersion of NSB measurements over the course of a night is typically 0.2 mag, based upon our SQM data.

We investigate the long term variations of the NSB and its correlation with solar activity. We find a trend of decreasing NSB with decreasing solar activity in the UBV and SQM bands, though the trend is statistically robust only for the UB and SQM bands, perhaps due to too few data points in the VR bands.

We compare the NSB at the OAN-SPM with measurements made elsewhere and find that the NSB at the OAN-SPM is comparable to that of other observing sites. When comparing data from different observatories, we find a strong correlation between the NSB and the solar flux at the time the measurements were made,

which can be useful to estimate the expected increase in the NSB due to solar activity for any site. The variation in the NSB due to solar activity can be as high as 0.6 and 0.9 mag (B and V bands) from the maximum (250 sfu) to the minimum (60 sfu) of the solar cycle. The NSB data presented here should be useful for long-term monitoring of the quality of OAN-SPM site, which remains one of the darkest sites in use and for future large telescope facilities.

This work is based upon observations carried out at the Observatorio Astronómico Nacional on the Sierra San Pedro Mártir (OAN-SPM), Baja California, México. We thank the daytime and night support staff at the OAN-SPM for facilitating and helping obtain our observations. I. P-F. would like to thank L. Gutiérrez, M. Núñez, F. Murillo, M. Murillo, J. L. Ochoa, F. Quiros, H. Serrano, C. Tejada, D. Clark, L. Fox, T. Verdugo, C. Durán, G. Guisa, E. López, B. García, B. Martínez, F. Guillén, G. Melgoza, S. Monrroy, and F. Montalvo.

REFERENCES

- Abreu, V. J., Skinner, W. R., and Hays, P. B. 1980, *Geophys. Res. Lett.*, 7, 109
- Benn, C. R. and Ellison, S. L. 1998, *New A Rev.*, 42, 503
- Cinzano, P. 2005, *ISTIL Internal Report*, 9

- Echevarría, J., Tapia, M., Costero, R., Salas, L., Michel, R., Rojas, M. A., Muñoz, R., Valdez, J., Ochoa, J. L., Palomares, J., Harris, O., Cromwell, R. H., Woolf, N. J., Persson, S. E., and Carr, D. M. 1998, *Rev. Mexicana Astron. Astrofis.*, 34, 47
- Garstang, R. H. 1989, *PASP*, 101, 306
- Kalinowski, J. K., Roosen, R. G., and Brandt, J. C. 1975, *PASP*, 87, 869
- Krisciunas, K. 1990, *PASP*, 102, 1052
- Krisciunas, K. 1997, *PASP*, 109, 1181
- Krisciunas, K., Sinton, W., Tholen, K., Tokunaga, A., Golisch, W., Griep, D., Kaminski, C., Impey, C., and Christian, C. 1987, *PASP*, 99, 887
- Laher, R. R., Gorjian, V., Rebull, L. M., Masci, F. J., Fowler, J. W., Helou, G., Kulkarni, S. R., and Law, N. M. 2012, *PASP*, 124, 737
- Landolt, A. U. 1992, *AJ*, 104, 340
- Leinert, C., Vaisanen, P., Mattila, K., and Lehtinen, K. 1995, *A&AS*, 112, 99
- Levasseur-Regourd, A. C. and Dumont, R. 1980, *A&A*, 84, 277
- Mattila, K., Vaisanen, P., and Appen-Schnur, G. F. O. V. 1996, *A&AS*, 119, 153
- Michel, R., Echevarría, J., Costero, R., and Harris, O. 2003, *Rev. Mexicana Astron. Astrofis.*, 19, 37
- Patat, F. 2003, *A&A*, 400, 1183
- Pilachowski, C. A., Africano, J. L., Goodrich, B. D., and Binkert, W. S. 1989, *PASP*, 101, 707
- Rayleigh, L. 1929, *Proceedings of the Royal Society of London Series A*, 119, 11
- Rayleigh, L. and Jones, H. S. 1935, 151, 222
- Sánchez, L. J., Cruz-González, I., Echevarría, J., Ruelas-Mayorga, A., García, A. M., Avila, R., Carrasco, E., Carramiñana, A., and Nigoche-Netro, A. 2012, *MNRAS*, 426, 635
- Schneeberger, T. J., Worden, S. P., and Beckers, J. M. 1979, *PASP*, 91, 530
- Schuster, W. J. and Parrao, L. 2001, *Rev. Mexicana Astron. Astrofis.*, 37, 187
- Skidmore, W., Els, S., Travouillon, T., Riddle, R., Schöck, M., Bustos, E., Seguel, J., and Walker, D. 2009, *PASP*, 121, 1151
- Takahashi, H., Sahai, Y., and Batista, P. P. 1984, *Planet. Space Sci.*, 32, 897
- Tapia, M., Cruz-González, I., Hiriart, D., and Richer, M. 2007, *Rev. Mexicana Astron. Astrofis.*, 31, 47
- Walker, M. F. 1988, *PASP*, 100, 496
- Yee, J. H., Abreu, V. J., and Hays, P. B. 1981, *J. Geophys. Res.*, 86, 1564

APPENDIX

MEASUREMENTS OF CCD NIGHT SKY BRIGHTNESS

Table 7 presents all of the NSB measurements made using CCD images from 18 nights during the years 2013-2016. Columns 1 and 2 are the UT date and time of the measurements. Cols. 3-7 present the NSB measurements in the UBVRI bands, respectively, uncorrected for the contribution of the zodiacal light. In parentheses in these columns, we present the correction for zodiacal light for each individual measurement. Column 8 presents the “observed” solar 10.7 cm flux measured on the previous UT date of the measurement. Figure 12 presents these data as a function of the solar 10.7 cm flux.

MEASUREMENTS OF SQM NIGHT SKY BRIGHTNESS

Table 8 presents all of the NSB measurements made with the SQM sensor for 183 clear nights during dark time from November 2014 to June 2016. Column 1 is the UT date, Col. 2 the mean NSB, uncorrected for the contribution of the zodiacal light, Col. 3 the standard deviation of the measurements, Cols. 4 and 5 the minimum NSB and maximum NSB, respectively, Col. 6 is the number of measurements (one per minute), and Col. 7 is the zodiacal light correction.

TABLE 7
CCD NIGHT SKY BRIGHTNESS AT OAN-SPM

UT Date	UT (hh:mm)	NSB _U (Δ ZL)	NSB _B (Δ ZL)	NSB _V (Δ ZL)	NSB _R (Δ ZL)	NSB _I (Δ ZL)	Flux _☉ ^a
2013							
18 Feb	10:29	22.47(0.37)	22.81(0.48)	22.11(0.24)	21.17(0.13)	19.87(0.03)	107
2 Apr	04:05	21.96(0.50)	22.37(0.64)	21.35(0.32)	20.55(0.18)	18.88(0.05)	120
2014							
28 Jan	11:07	22.41(0.38)	22.65(0.48)	21.76(0.24)	21.16(0.13)	19.44(0.03)	142
29 Mar	04:45	22.02(0.50)	22.05(0.61)	21.09(0.31)	20.41(0.19)	18.82(0.05)	147
24 Apr	04:29	22.14(0.48)	22.45(0.60)	21.41(0.31)	20.86(0.17)	19.52(0.05)	134
15 Sep	05:28	21.67(0.33)	22.62(0.44)	21.95(0.21)	20.57(0.11)	19.68(0.03)	140
28 Oct	09:11	21.56(0.37)	22.20(0.47)	21.05(0.23)	20.36(0.13)	18.99(0.03)	182
2015							
17 Mar	08:10	22.29(0.45)	22.82(0.55)	21.64(0.29)	21.24(0.16)	19.70(0.04)	117
17 Jun	05:33	22.01(0.32)	22.46(0.42)	21.61(0.19)	21.14(0.10)	19.35(0.03)	136
8 Aug	06:23	22.58(0.53)	22.53(0.41)	21.61(0.26)	20.91(0.14)	19.41(0.04)	122
3 Oct	03:22	22.27(0.30)	22.61(0.40)	21.57(0.19)	20.95(0.10)	19.31(0.03)	105
2016							
15 Jan	09:24	22.47(0.50)	22.72(0.64)	21.80(0.32)	21.08(0.18)	19.23(0.05)	104
26 Jan	02:54	22.15(0.56)	22.40(0.69)	21.34(0.35)	20.49(0.20)	18.89(0.05)	107
12 Mar	08:53	22.81(0.45)	22.66(0.55)	21.63(0.29)	20.94(0.16)	18.94(0.04)	95
9 Apr	09:39	22.65(0.35)	22.96(0.46)	21.92(0.21)	21.37(0.12)	19.90(0.03)	101
12 May	11:14	22.84(0.32)	23.26(0.40)	21.95(0.21)	21.46(0.10)	19.81(0.03)	92
27 May	06:41	22.52(0.28)	22.64(0.41)	21.33(0.19)	20.83(0.14)	19.29(0.03)	89
28 May	04:57	22.12(0.35)	22.57(0.45)	21.52(0.21)	20.66(0.11)	18.81(0.03)	91

Units are mag arcsec⁻². Δ ZL is the correction for zodiacal light.

Units are 1 sfu = 10⁴ Jy = 10⁻²² W m⁻² Hz⁻¹.

^a Solar flux measurements are the last values reported from the previous UT date.

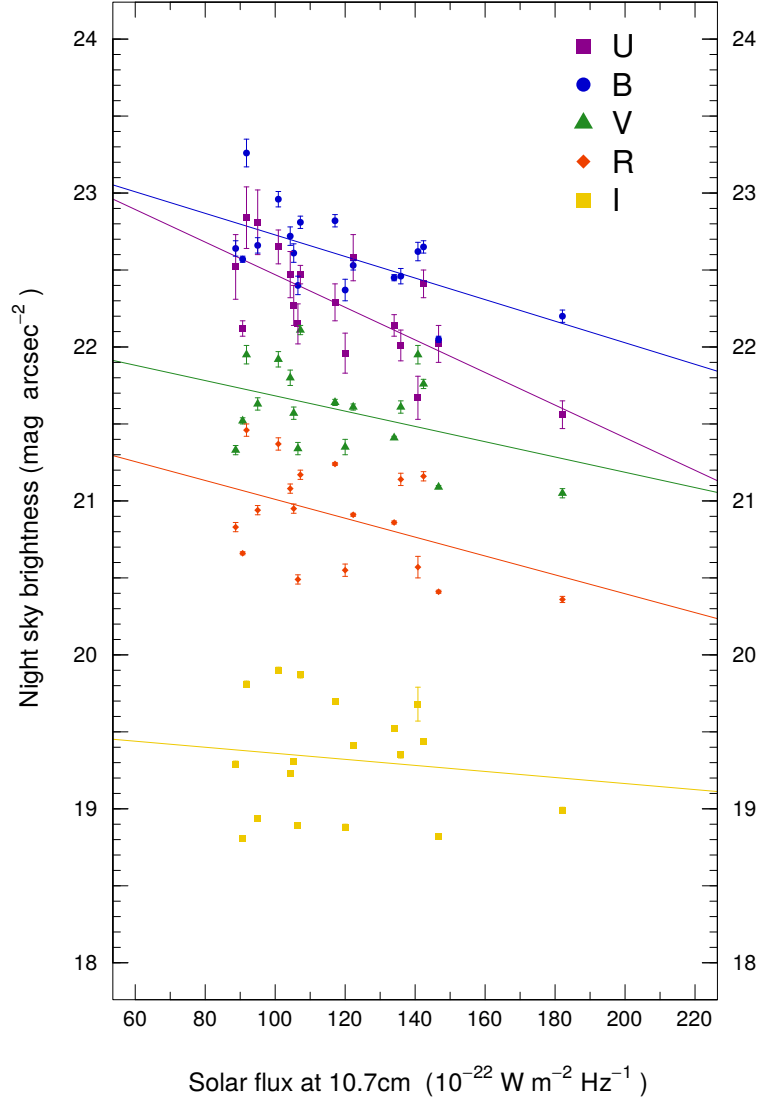


FIG. 12.— Distribution of the NSB in the UBVRI filters for 18 nights from 2013 to 2016. The abscissa values are the solar 10.7 cm flux measured on the date of the measurement. The NSB values are not corrected for zodiacal light (see Table 7).

TABLE 8 SQM Night sky brightness at OAN-SPM

UT Date	NSB	σ	NSB _{min}	NSB _{max}	N	ΔZL
2014-11-03	21.30	0.000	21.30	21.30	15	0.39
2014-11-12	21.50	0.022	21.46	21.54	57	0.26
2014-11-13	21.52	0.031	21.45	21.57	117	0.26
2014-11-16	21.51	0.037	21.40	21.55	287	0.29
2014-11-17	21.52	0.032	21.46	21.59	316	0.30
2014-11-18	21.45	0.043	21.33	21.50	316	0.30
2014-11-20	21.53	0.037	21.43	21.57	306	0.29
2014-11-22	21.51	0.100	21.36	21.68	396	0.31
2014-11-23	21.41	0.126	21.23	21.61	363	0.31
2014-11-26	21.26	0.017	21.23	21.30	190	0.34
2014-11-27	21.31	0.014	21.25	21.33	133	0.33
2014-11-28	21.30	0.010	21.27	21.32	131	0.33
2014-11-29	21.37	0.019	21.34	21.40	134	0.33
2015-01-16	21.44	0.024	21.40	21.48	162	0.36
2015-01-17	21.42	0.063	21.36	21.53	220	0.35
2015-01-18	21.45	0.064	21.36	21.58	273	0.34
2015-01-19	21.53	0.133	21.37	21.77	329	0.32
2015-01-20	21.55	0.118	21.40	21.75	385	0.31
2015-02-11	21.40	0.000	21.40	21.40	11	0.35
2015-02-12	21.36	0.008	21.34	21.38	72	0.33
2015-02-13	21.39	0.040	21.34	21.46	131	0.34
2015-02-16	21.53	0.121	21.36	21.70	309	0.32
2015-02-17	21.47	0.102	21.32	21.62	369	0.31
2015-02-18	21.63	0.153	21.39	21.81	422	0.30
2015-02-24	21.66	0.043	21.59	21.73	235	0.25
2015-02-26	21.71	0.027	21.67	21.74	113	0.22
2015-03-13	21.45	0.054	21.39	21.61	166	0.32
2015-03-22	21.64	0.090	21.42	21.79	408	0.26
2015-03-23	21.63	0.082	21.46	21.74	339	0.25
2015-03-24	21.76	0.043	21.64	21.82	271	0.24
2015-03-25	21.57	0.041	21.50	21.64	208	0.23
2015-03-26	21.58	0.020	21.55	21.62	151	0.21
2015-03-27	21.67	0.052	21.55	21.73	99	0.20
2015-03-28	21.73	0.039	21.67	21.79	53	0.19
2015-04-10	21.61	0.083	21.48	21.73	104	0.32
2015-04-13	21.38	0.055	21.26	21.50	250	0.28
2015-04-14	21.50	0.051	21.33	21.58	298	0.28
2015-04-15	21.66	0.066	21.46	21.72	344	0.27
2015-04-16	21.63	0.084	21.40	21.75	385	0.26
2015-04-17	21.62	0.050	21.43	21.69	421	0.26
2015-04-18	21.61	0.063	21.43	21.70	461	0.25
2015-04-20	21.62	0.073	21.36	21.68	375	0.23
2015-04-21	21.65	0.114	21.35	21.76	307	0.23
2015-04-22	21.60	0.072	21.42	21.69	245	0.22
2015-05-09	21.72	0.024	21.68	21.75	55	0.29
2015-05-10	21.63	0.040	21.57	21.68	102	0.28
2015-05-12	21.69	0.051	21.62	21.79	191	0.26
2015-05-13	21.67	0.062	21.55	21.75	235	0.25
2015-05-16	21.64	0.067	21.45	21.74	349	0.23
2015-05-18	21.61	0.120	21.34	21.74	362	0.22
2015-05-19	21.69	0.084	21.43	21.79	306	0.21
2015-05-20	21.56	0.086	21.35	21.68	244	0.20
2015-05-23	21.57	0.096	21.39	21.71	95	0.19
2015-05-24	21.43	0.022	21.38	21.45	55	0.19
2015-05-25	21.44	0.024	21.40	21.48	17	0.19
2015-06-08	21.92	0.017	21.89	21.95	51	0.21
2015-06-11	21.62	0.023	21.57	21.65	165	0.20
2015-06-12	21.64	0.060	21.49	21.72	205	0.20
2015-06-13	21.60	0.116	21.29	21.72	239	0.20
2015-06-14	21.66	0.135	21.36	21.81	235	0.20
2015-06-15	21.64	0.132	21.43	21.85	230	0.20
2015-06-16	21.63	0.082	21.42	21.77	226	0.20
2015-06-17	21.76	0.116	21.52	21.92	213	0.20
2015-06-18	21.69	0.125	21.43	21.84	160	0.19
2015-06-19	21.45	0.082	21.33	21.58	112	0.19
2015-06-20	21.66	0.064	21.55	21.77	71	0.19

TABLE 8 continued.

UT Date	NSB	σ	NSB_{\min}	NSB_{\max}	N	ΔZL
2015-06-21	21.62	0.038	21.56	21.69	32	0.19
2015-07-07	21.81	0.007	21.80	21.82	10	0.19
2015-07-08	21.82	0.021	21.77	21.84	46	0.19
2015-07-12	21.67	0.115	21.45	21.86	125	0.19
2015-07-13	21.54	0.087	21.38	21.65	121	0.19
2015-07-14	21.68	0.091	21.52	21.80	119	0.19
2015-07-15	21.53	0.100	21.36	21.69	138	0.20
2015-07-16	21.74	0.077	21.57	21.83	158	0.21
2015-07-17	21.69	0.077	21.52	21.78	140	0.22
2015-07-21	21.75	0.014	21.72	21.77	71	0.26
2015-07-22	21.62	0.017	21.57	21.64	75	0.26
2015-07-23	21.74	0.018	21.70	21.76	80	0.26
2015-07-24	21.47	0.040	21.41	21.52	85	0.26
2015-07-25	21.75	0.038	21.69	21.83	91	0.26
2015-07-26	21.73	0.024	21.69	21.75	58	0.26
2015-07-27	21.93	0.006	21.92	21.94	15	0.28
2015-08-07	21.63	0.058	21.55	21.74	47	0.19
2015-08-08	21.54	0.034	21.48	21.59	44	0.19
2015-08-09	21.58	0.040	21.52	21.64	40	0.19
2015-08-10	21.46	0.032	21.41	21.51	38	0.19
2015-08-13	21.83	0.144	21.55	22.02	154	0.25
2015-08-14	21.80	0.154	21.40	21.92	212	0.26
2015-08-15	21.86	0.124	21.52	22.00	215	0.26
2015-08-18	21.73	0.051	21.64	21.81	207	0.27
2015-08-19	21.78	0.028	21.68	21.82	212	0.27
2015-08-20	21.77	0.051	21.65	21.85	216	0.27
2015-08-21	21.82	0.047	21.72	21.87	221	0.27
2015-08-22	21.95	0.039	21.85	22.00	208	0.27
2015-08-23	21.84	0.028	21.76	21.88	168	0.28
2015-08-24	21.89	0.017	21.84	21.91	118	0.29
2015-09-13	21.61	0.047	21.50	21.69	320	0.29
2015-09-14	21.59	0.037	21.52	21.65	321	0.29
2015-09-15	21.54	0.051	21.43	21.64	318	0.29
2015-09-16	21.70	0.079	21.10	21.79	318	0.29
2015-09-17	21.70	0.049	21.58	21.76	321	0.29
2015-09-19	21.73	0.035	21.64	21.79	277	0.29
2015-10-05	21.41	0.009	21.40	21.43	52	0.26
2015-10-06	21.51	0.026	21.48	21.56	174	0.26
2015-10-17	21.47	0.024	21.42	21.50	496	0.32
2015-10-19	21.56	0.049	21.46	21.63	280	0.33
2015-11-02	21.52	0.015	21.50	21.56	64	0.26
2015-11-03	21.48	0.013	21.46	21.51	126	0.26
2015-11-05	21.43	0.020	21.37	21.47	245	0.29
2015-11-06	21.52	0.044	21.41	21.58	302	0.30
2015-11-07	21.52	0.044	21.40	21.57	326	0.30
2015-11-08	21.44	0.058	21.35	21.54	326	0.30
2015-11-09	21.39	0.052	21.29	21.47	326	0.30
2015-11-10	21.42	0.037	21.34	21.48	326	0.30
2015-11-11	21.35	0.096	21.11	21.48	361	0.31
2015-11-12	21.41	0.076	21.19	21.47	362	0.31
2015-11-13	21.44	0.083	21.26	21.55	318	0.32
2015-11-14	21.49	0.121	21.30	21.67	274	0.33
2015-11-18	21.45	0.036	21.39	21.50	83	0.36
2015-11-19	21.44	0.010	21.42	21.45	87	0.36
2015-11-20	21.43	0.058	21.32	21.51	90	0.36
2015-11-21	21.57	0.020	21.53	21.61	94	0.35
2015-12-02	21.68	0.023	21.63	21.71	154	0.27
2015-12-06	21.53	0.042	21.46	21.61	247	0.29
2015-12-09	21.50	0.084	21.37	21.64	300	0.30
2015-12-13	21.48	0.056	21.40	21.60	320	0.32
2015-12-15	21.37	0.049	21.31	21.45	208	0.32
2015-12-16	21.44	0.047	21.36	21.50	211	0.32
2015-12-17	21.42	0.022	21.37	21.47	216	0.32
2015-12-18	21.48	0.026	21.41	21.52	220	0.32
2016-01-03	21.54	0.014	21.52	21.57	122	0.32
2016-01-09	21.58	0.082	21.44	21.69	372	0.32
2016-01-12	21.62	0.038	21.52	21.68	326	0.31

TABLE 8 continued.

UT Date	NSB	σ	NSB _{min}	NSB _{max}	N	ΔZL
2016-01-15	21.73	0.065	21.52	21.81	319	0.30
2016-01-16	21.70	0.037	21.65	21.77	251	0.29
2016-02-05	21.66	0.026	21.59	21.73	248	0.34
2016-02-06	21.58	0.108	21.37	21.74	303	0.33
2016-02-07	21.69	0.082	21.50	21.82	355	0.32
2016-02-08	21.62	0.099	21.46	21.86	408	0.31
2016-02-09	21.80	0.142	21.52	22.00	425	0.30
2016-02-12	21.85	0.061	21.77	21.95	740	0.29
2016-02-13	21.70	0.052	21.64	21.82	608	0.28
2016-02-15	21.63	0.010	21.61	21.66	332	0.25
2016-02-16	21.44	0.028	21.40	21.50	208	0.23
2016-02-17	21.49	0.014	21.46	21.50	92	0.21
2016-03-07	21.83	0.084	21.61	21.95	426	0.30
2016-03-10	21.71	0.037	21.64	21.82	481	0.27
2016-03-13	21.77	0.029	21.71	21.82	271	0.25
2016-03-15	21.84	0.021	21.81	21.87	138	0.21
2016-03-16	21.91	0.027	21.85	21.95	85	0.20
2016-03-17	21.82	0.019	21.79	21.85	36	0.20
2016-03-29	21.65	0.039	21.58	21.70	91	0.33
2016-03-30	21.74	0.026	21.69	21.79	143	0.32
2016-04-01	21.70	0.045	21.61	21.79	241	0.30
2016-04-02	21.74	0.098	21.57	21.90	288	0.29
2016-04-03	21.66	0.057	21.55	21.76	334	0.28
2016-04-04	21.76	0.112	21.62	21.93	379	0.28
2016-04-13	21.81	0.066	21.64	21.88	117	0.20
2016-04-15	21.53	0.025	21.49	21.57	25	0.19
2016-04-27	21.64	0.027	21.59	21.69	44	0.31
2016-04-28	21.68	0.049	21.57	21.74	180	0.28
2016-04-30	21.65	0.046	21.55	21.72	372	0.27
2016-05-03	21.82	0.073	21.61	21.87	310	0.25
2016-05-04	21.75	0.031	21.64	21.79	346	0.25
2016-05-09	21.60	0.107	21.35	21.72	255	0.21
2016-05-10	21.62	0.075	21.42	21.70	191	0.20
2016-05-13	21.56	0.037	21.50	21.61	45	0.19
2016-05-27	21.80	0.008	21.79	21.82	39	0.26
2016-05-28	21.83	0.008	21.82	21.84	80	0.24
2016-05-29	21.75	0.037	21.69	21.82	120	0.23
2016-05-30	21.79	0.015	21.76	21.81	161	0.22
2016-05-31	21.83	0.064	21.70	21.91	196	0.22
2016-06-01	21.82	0.023	21.74	21.86	235	0.21
2016-06-02	21.81	0.107	21.55	21.94	276	0.21
2016-06-03	21.87	0.099	21.61	22.00	281	0.20
2016-06-04	21.89	0.112	21.62	22.01	276	0.20
2016-06-05	21.90	0.150	21.50	22.03	271	0.20
2016-06-07	21.74	0.130	21.47	21.91	161	0.19
2016-06-08	21.72	0.072	21.59	21.84	107	0.19
2016-06-09	21.67	0.065	21.55	21.77	62	0.19
2016-06-10	21.53	0.011	21.51	21.54	20	0.19
2016-06-26	21.94	0.003	21.93	21.94	28	0.21
2016-06-28	21.98	0.048	21.88	22.04	105	0.20